Membrane Water Treatment, Vol. 4, No. 2 (2013) 127-142
DOI: http://dx.doi.org/10.12989/mwt.2013.4.2.127

Dehydration and pore swelling effects on the transfer of PEG through NF membranes

Aurélie Escoda[1], Saliha Bouranene[2], Patrick Fievet[*1], Sébastien Déon[1] and Anthony Szymczyk[3]

[1]*Institut UTINAM, Université de Franche-Comté, 25030 Besançon cedex, France*
[2]*Université Mohamed Chérif Messaadia, Souk-Ahras, 41000, Algérie*
[3]*Université de Rennes1, Institut des Sciences Chimiques de Rennes, 35042 France*

(Received June 12, 2012, Revised January 18, 2013, Accepted March 15, 2013)

Abstract. In order to investigate the significance of "salting-out" and "pore swelling" effects on the nanofiltration of neutral solutes, rejection properties of two NF ceramic and polymeric membranes were studied with single polyethyleneglycol (PEG) solution and mixed PEG/inorganic electrolyte solutions. For both membranes, the rejection rate of PEG was found to decrease significantly in the presence of ions. In the case of the ceramic membrane (rigid pores), this phenomenon was imputed to the sole partial dehydration of PEG molecules induced by the surrounding ions. This assumption was confirmed by the lowering of the PEG rejection rates which followed the Hofmeister series. Experimental data were used to compute the resulting decrease in the Stokes radius of PEG molecules in the presence of the various salts. Concerning the polymeric membrane, the decrease in the rejection rate was found to be systematically higher than for the ceramic membrane. The additional decrease was then ascribed to the swelling of the pores. The experimental data of rejection rates were then used to compute the variation in the mean pore radius in the presence of the various salts. The pore swelling phenomenon due to accumulation of counterions inside pores was supported by electrokinetic charge density measurements.

Keywords: dehydration; salting-out; hofmeister effects; pore swelling; nanofiltration; ceramic membrane; organic membrane; salts; streaming potential

1. Introduction

Nanofiltration (NF) has attracted increasing attention over the recent years due to its real application potential for the separation or purification of complex liquid mixtures. However, its development is hindered because of the difficulty to predict its performances when the fluid composition varies. This difficulty could be overcome providing a better understanding of the mechanisms that rule the transfer of the solutes through NF membranes. Some recent studies have shown that the transfer of an organic solute increases in the presence of a salt (Bouchoux 2005, Bargeman 2005, Bouranene 2007, Mandale 2008, Luo 2011) and that this increase also depends on the salt nature and its concentration. Organic solutes such as saccharides (glucose, sucrose, raffinose…), glycerol, benzyl alcohol, sodium benzoate, glutamic acid, iminodiacetic acid,

*Corresponding author, Professor, E-mail: patrick.fievet@univ-fcomte.fr

caffeine… in the presence of inorganic salts such as NaCl, $CaCl_2$, $MgCl_2$, Na_2SO_4, Na_2HPO_4…were filtrated. Several hypotheses have been suggested to explain the decrease in the solute rejection in the presence of salts. These ones are:

- The partial dehydration of the molecules by the surrounding ions (Bouchoux 2005, Bouranene 2007) leading to a decrease in their effective size. This phenomenon is referred as the "salting-out" effect or "Hofmeister" effect from the author's name who firstly observed the effect of salt nature on the precipitation of hen-egg-white protein (Kunz 2004). In order to give a survey of the large differences between the precipitation effects of the individual salts, ions were ranked according to their efficiency. The sequences so-obtained for cations and anions, called "Hofmeister series", are therefore a classification of ions towards their ability to favor precipitation (salting-out) or solubility (salting-in) of proteins. Nowadays, the salting-out effect indicates a very general phenomenon, in which the solubility of a solute in water is decreased when salt is added (the opposite effect is known as salting-in effect). The Hofmeister effect is probably the most well-known effect attributed to structure-making and -breaking character of ions. The competition between ions and PEG for water in confined spaces, such as nanopores, could be one possible reason for Hofmeister effect (or salting-out effect). Indeed, if water inside nanopores preferentially solvates ions to the detriment of the molecules, the latter, therefore less hydrated, might have a smaller effective volume than that in the absence of salts and then, an increased transfer through the membrane pores (Bouchoux 2005).
- The increase in the mean pore size (phenomenon referred as "pore swelling") due to the increase of the membrane charge by adding salt (this increased charge would lead to an increase of the number of counterions inside pores and thus, to a stronger repulsive interactions) (Bouchoux 2005, Bargeman 2005).
- The increase in the mean pore size due to the thinning of the hydration layer at the pore surface resulting from the salting-out effect (Luo 2011).
- The stronger reduction of the flux through small pores as compared with larger pores leading to more organic solutes passing through larger pores, which would determine the rejection (Bargeman 2005).
- The opening of the membrane pores due to the compression of the electrical double layer formed at the membrane surface (Mandale 2008).
- The increase of the effective membrane thickness due to collisions between ions and neutral solutes, which would lengthen the moving path of solutes. However, it should be noted that this assumption cannot explain the decrease of the limiting rejection rate of neutral solutes since the limiting rejection does not depend on the effective membrane thickness (Luo 2011).
- The change in molecular polarity of solutes (Mandale 2008).

The aim of this work was to evaluate the significance of pore swelling and/or salting-out effects in the case of NF ceramic and polymeric membranes and a model system: a mixture of polyethyleneglycol (PEG) and salt.

2. Theory

2.1 Rejection rate of neutral solutes

The model used to describe the solute transport through NF membranes has been presented in detail in many papers (Bouranene 2007). That is why only a brief description of the model will be

made in this section. For the mathematical derivation of the model, the following assumptions have been considered:

- The membrane consists of a bundle of identical cylindrical pores of radius r_p and length Δx with $\Delta x >> r_p$ so that both solute and volume fluxes can be considered one-dimensional.
- The size of solutes is expressed as a Stokes radius ($r_{i,s}$) and is calculated from the diffusion coefficient ($D_{i,\infty}$), with the Stokes-Einstein equation (Eq. (7) in Table 1).
- The solute and volume fluxes are defined in terms of radially averaged quantities.
- The volume flux is fully developed inside the pore and has a parabolic profile of the Hagen-Poiseuille type.

The main equations used for the model are summarised in Table 1.The model is based on the application of the extended Nernst-Planck equation to describe the transport of solutes through the membrane (Eq. (1)). The terms on the RHS of this equation represent transport due to diffusion and convection, respectively. $K_{i,d}$ and $K_{i,c}$ are the hindrance factors for the diffusion and convection, accounting for the effect of finite solute and pore sizes on the diffusive and convective components of solute transport. For purely steric exclusion mechanism between solute and cylindrical pores, the solute partitioning coefficient at both membrane/solution interfaces is given by Eq. (6). Integrating Eq. (1) across the membrane thickness (i.e., from $x = 0$ to $x = \Delta x$) while considering the filtration condition (Eq. (8)) gives the expression for the intrinsic rejection rate (Eq. (9)). The intrinsic rejection rate is independent of the concentration polarization phenomenon (Zydney 1997) and thus characterizes the real performance of the membrane. As shown by Eq. (9), the intrinsic rejection rate of neutral solutes, at a given filtration flux J_v, is a function of two parameters, λ_i and $\Delta x/A_k$. It increases with J_v and reaches a limiting value of $1 - \phi_i K_{i,c}$ at infinite J_v (Eq. (10)), which only depends on λ_i.

For a neutral solute solution, the intrinsic rejection rate is related to the observed rejection rate by Eq. (12) (Table 1). The observed rejection rate, which depends on the concentration polarization phenomenon, corresponds to an experimentally measured value unlike the intrinsic rejection rate which can be only computed. The mass-transfer coefficient k in Eq. (13) can be assessed from a Sherwood correlation (Eq. (14)).

Table 1 Summary of equations used in the model (all symbols are defined in the nomenclature section)

ENP equation

$$j_i = -K_{i,d} D_{i,\infty} \frac{dc_i}{dx} + K_{i,c} c_i \frac{J_v}{A_k} \tag{1}$$

Steric hindrance factors

$$K_{i,d} = \frac{6\pi}{K_{i,t}} \tag{2}$$

$$K_{i,c} = \frac{(2 - \phi_i) K_{i,s}}{2 K_{i,t}} \tag{3}$$

Table 1 Continued

Hydrodynamic drag coefficients

$$K_{i,t} = \frac{9}{4}\pi^2\sqrt{2}\left(1-\lambda_i\right)^{-5/2}\left[1+\sum_{n=1}^{2}a_n\left(1-\lambda_i\right)^n\right]+\sum_{n=0}^{4}a_{n+3}\lambda^n \tag{4}$$

$$K_{i,s} = \frac{9}{4}\pi^2\sqrt{2}\left(1-\lambda_i\right)^{-5/2}\left[1+\sum_{n=1}^{2}b_n\left(1-\lambda_i\right)^n\right]+\sum_{n=0}^{4}b_{n+3}\lambda^n \tag{5}$$

with $a_1 = -73/60$, $a_2 = 77.293/50.400$, $a_3 = -22.5083$, $a_4 = -5.6117$, $a_5 = -0.3363$, $a_6 = -1.216$, $a_7 = 1.647$, $b_1 = 7/60$, $b_2 = -2.227/50.400$, $b_3 = 4.0180$, $b_4 = -3.9788$, $b_5 = -1.9215$, $b_6 = 4.392$, $b_7 = 5.006$.

Steric partitioning coefficient

$$\frac{c_i(0^+)}{c_{i,m}} = \frac{c_i(\Delta x^-)}{c_{i,p}} = \phi_i = \left(1-\frac{r_{i,s}}{r_p}\right)^2 \tag{6}$$

with

$$r_{i,s} = \frac{\mathrm{k_B}T}{6\pi\eta D_{i,\infty}} \tag{7}$$

Filtration condition

$$j_i = J_v\, c_{i,p} / A_k \tag{8}$$

Intrinsic and observed rejection rates

$$R_{\mathrm{int}} = 1-\frac{c_{i,p}}{c_{i,m}} = 1-\frac{\phi_i K_{i,c}}{1-\left[\left(\exp\left(-\frac{K_{i,c}J_v\Delta x}{K_{i,d}D_{i,\infty}A_k}\right)\right)\left(1-\phi_i K_{i,c}\right)\right]} \tag{9}$$

$$R_{\mathrm{lim,int}} = 1-\phi_i K_{i,c} \tag{10}$$

$$R_{obs} = 1-\frac{c_{i,p}}{c_{i,f}} \tag{11}$$

$$R_{\mathrm{int}} = \frac{R_{obs}\exp\left(J_v/k\right)}{1-R_{obs}\left(1-\exp\left(J_v/k\right)\right)} \tag{12}$$

with

$$k = \frac{D_{i,\infty}}{\delta} \tag{13}$$

Sherwood correlation

$$Sh = kd_h / D_{i,\infty} = \alpha_1\,\mathrm{Re}^{\alpha_2}\,Sc^{\alpha_3} \tag{14}$$

2.2 Electrokinetic charge density

The zeta-potential is a parameter directly related to the electrokinetic charge density. Streaming potential is the most commonly used tool for determining the zeta-potential of membranes. Measurements of streaming potential can be performed in a transversal or tangential mode. In the case of NF membranes, it is advisable to use the second mode (Labbez 2001, Yaroshchuk 2002). The tangential streaming potential (TSP) technique consists in applying a pressure difference across a thin channel formed by two identical membrane samples facing one another and separated by a spacer. Cell electric conductance measurements allow taking into account the possible contribution of the membrane porous body to the conduction phenomenon during the streaming potential process. The zeta-potential can then be determined using the following relation

$$\zeta = \frac{\Delta\varphi_s}{\Delta P} G_t \frac{\eta}{\varepsilon_0 \varepsilon_r} \left(\frac{l}{2\mathrm{h}\ L_c} \right) \tag{15}$$

where $\Delta\varphi_s$ is the streaming potential, ΔP the pressure difference between the ends of the channel, G_t the total conductance of the membrane/channel/membrane sandwich, ε_0 the vacuum permittivity, ε_r the relative dielectric constant of the solvent, η its dynamic viscosity, 2 h the channel height, L_c its width and l its length.

The zeta-potential is related to the electrokinetic charge density σ_{ek} (expressed in $C\ m^{-2}$) as follows (Hunter 1881)

$$\sigma_{ek} = -sign(\zeta) \sqrt{\left[2\varepsilon_r \varepsilon_0 RT \sum_i c_{i,f} \left[\exp\left(\frac{-z_i F \zeta}{RT} \right) - 1 \right] \right]} \tag{16}$$

where $c_{i,f}$ is the concentration of ion i in the feed solution.

Here, we assume that the charge density inside pores is the same as the external charge density estimated from TSP measurements and Eq. (16).

3. Experimental

3.1 Membranes

Filtration experiments were performed with two commercial NF membranes: a flat thin-film composite membrane with a polyamide top layer on a polyester support (labeled Desal GH and produced by GE Osmonics) and a TiO_2 tubular membrane composed of three identical channels in clover of length 604 mm and cross-section area 11 mm^2 (labeled Filtanium and produced by TAMI-Industries). According to the suppliers, the molecular weight cut-offs (MWCO) of Desal GH and Filtanium membranes are 2500 and 1000 Da, respectively. Pure water permeability of 3.3 $L\ h^{-1}\ m^{-2}\ bar^{-1}$ is also provided for Desal GH.

3.2 Chemicals

Polyethyleneglycol (PEG) with a molar mass of 600 $g\ mol^{-1}$(Fluka) and KCl, LiCl, $MgCl_2$ and K_2SO_4 salts of pure analytical grade (Prolabo) were used for experiments. Single-PEG and mixed

Table 2 Hydrodynamic conditions for filtration experiments performed with ceramic and polymeric membranes

	Ceramic membrane	Polymeric membrane
Transmembrane pressure ΔP (bars)	0.5-6	2-20
Hydraulic diameter d_h (mm)	3.6	0.51
Reynolds number *Re*	12000-40000	100-150
Schmidt number *Sc*	1600-2200	
Sherwood correlation	$Re = 0.0096Re^{0.91}Sc^{0.35}$	$Re = 0.2Re^{0.57}Sc^{0.4}$

PEG/salt solutions at a PEG concentration of 2 g L^{-1} were prepared with milli-Q quality water (conductivity < 1 μS cm^{-1}). The salt concentration in mixed-solute solutions was in the range 0.05-1 mol L^{-1} for rejection experiments and 0.0005-0.005 mol L^{-1} for electrokinetic measurements. The pH of solutions was 6.0 ± 0.2. The concentration of PEG in both feed and permeate solutions was determined from COD measurements and the salt concentration by conductivity measurements.

3.3 Filtration experiments

They were conducted under cross-flow conditions with the TAMILAB^R filtration unit for the ceramic membrane and the Osmonics Sepa CFII cell for the organic membrane. The filtration area was 220 and 140 cm^2 for the ceramic and polymeric membranes, respectively. The feed concentration was maintained constant by totally recycling the retentate and permeate. Rejection rates were measured as a function of the permeate volume flux by varying the transmembrane pressure. The working hydrodynamic conditions are given in Table 2.

3.4 Electrokinetic and electric measurements

TSP and conductance measurements were performed with a ZETACAD (CAD Inst., France) zeta-meter and a Solartron impedance spectrometer (1286 electrochemical interface and 1255 frequency response analyzer), respectively. The entire set-up and the exact measuring procedure can be found elsewhere (Fievet 2003). These measurements were only applied to the polymeric membrane. Samples of 50 × 30 mm, corresponding to the measuring cell, were cut in the sheet membrane. Experiments were conducted using a single channel height (2h), which was estimated from the channel hydraulic permeability by using Hagen-Poiseuille formula for slit channels (Szymczyk 2007).

4. Results and discussion

4.1 Determination of pore radius and thickness-to-porosity ratio using PEG

Fig. 1 shows an example of the intrinsic rejection rates of PEG 600 vs. permeate volume flux (J_v) for the ceramic and polymeric membranes. As expected, the rejection increases with J_v before leveling off at about 68% for the ceramic membrane and 90% for the polymeric one. As shown by

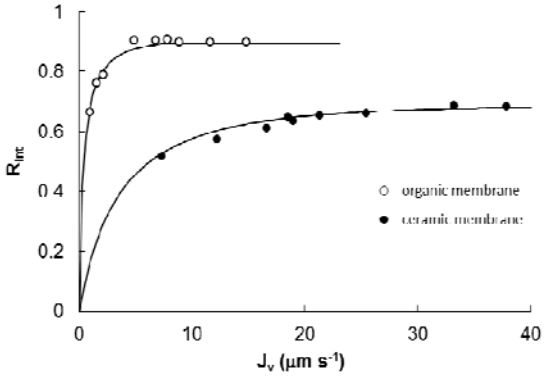

Fig. 1 Intrinsic rejection rate of PEG 600 vs. permeate volume flux for the ceramic and polymeric membranes. PEG feed concentration: 2 g L^{-1}; Symbols: experimental data; Full lines: intrinsic rejection rates computed from Eq. (9). $D_{PEG,\infty} = 3.14 \times 10^{-10}$ m^2 s^{-1}

Table 3 Effective pore radius (r_p) and thickness-to-porosity ratio ($\Delta x/A_k$) of ceramic and polymeric membranes determined from rejection data of PEG for a single-solute solution (PEG 400, 600 and 1000 g mol^{-1} for the ceramic membrane and PEG 600 for the polymeric one) and from a fitting procedure (Eq. (9))

	Ceramic membrane	Polymeric membrane
r_p (nm)	1.18 ± 0.04	0.875 ± 0.015
$\Delta x/A_k$ (μm)	3.92 ± 3.08	3.96 ± 0.74

the full lines, the data are well fitted by Eq. (9). Single-solute solutions of PEGs with different molar masses (400 and 1000 g mol^{-1}) were also filtrated through the ceramic membrane (results not shown). The effective pore radius and the ratio of the effective membrane thickness-to-porosity inferred from the fitting procedure are collected in Table 3. It appears that the ratio $\Delta x/A_k$ is almost identical for the two membranes and that the ceramic membrane (r_p = 1.18 nm) is a little more open than the polymeric one (r_p = 0.875 nm) by a factor 1.35, which is not consistent with the MWCOs provided by the manufacturers (Section 3.1). However, we do not know whether the same solute was used to determine the MWCO of ceramic and polymeric membranes and whether the MWCO was estimated at the same value of the solute rejection rate. It should be noted that a pore radius of 1.1 nm is obtained for the polymeric membrane by using the correlation established by Afonso *et al*. (2001) between the Stokes radii of PEGs and their respective molar mass, and considering the MWCO value for a PEG rejection of 90% (value of $R_{\lim,int}$ for the polymeric membrane).

4.2 Salt effects on PEG rejection in mixed-solute solutions

For both membranes, it was observed that rejection of PEG 600 is significantly lower in mixed-solute solutions (i.e., when a salt is present) than in single-solute solutions and that the decrease in the rejection rate increases with the salt concentration. Examples of the influence of the salt concentration on the PEG rejection by the ceramic and polymeric membranes are shown in Figs. 2(a) and (b), respectively. It should be noted that the rejection rate drop with increasing salt concentration, which was observed for all salts, cannot be ascribed to concentration polarization

effects since rejection rates are compared at identical permeate volume fluxes J_v (indeed, at different J_v, the concentration polarization would be different and then also the osmotic pressure would be different).

As illustrated by Figs. 3(a)-(c), the rejection rate of PEG also depends on the salt nature. By definition, a salt is composed of cations and anions. In order to discriminate between the effect of cations and anions on PEG rejection, salts with the same anion (KCl, $MgCl_2$ and LiCl) and salts with the same cation (KCl and K_2SO_4) were chosen. For the ceramic membrane, it is found that the decrease of the PEG rejection rates follows the Hofmeister series, i.e., $Mg^{2+} > Li^+ > K^+$ and $SO_4^{2-} > Cl^-$ at all concentrations whereas these sequences are not observed with the polymeric membrane (the drop in the rejection rate follows the sequence: $Li^+ > K^+ > Mg^{2+}$ and $SO_4^{2-} > Cl^-$ at 0.5 eq L^{-1}). Since pores of the ceramic membrane are rigid, the hypothesis of pore swelling can be eliminated with this membrane. The rejection rate drop is then ascribed to the partial dehydration of PEG molecules induced by surrounding ions. In order to investigate the influence of the salt nature on the dehydration effect, the mean r_p and $\Delta x/A_k$ values estimated from single-solute solutions were used to fit the rejection data of PEG in mixed-solute solutions, the Stokes radius of PEG 600 ($r_{PEG,s}$) being the single adjustable parameter.

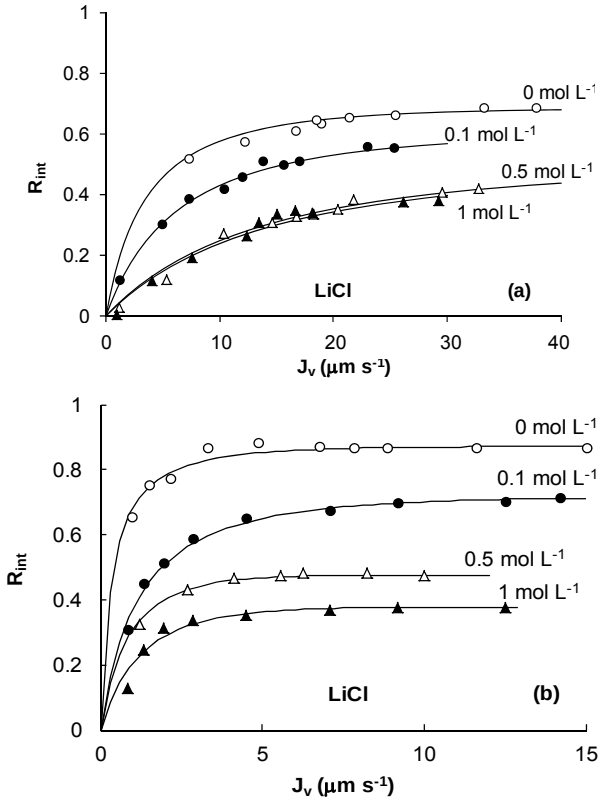

Fig. 2 Intrinsic rejection rate of PEG 600 vs. permeate volume flux for single-solute (PEG 600) and mixed-solute (PEG 600 + LiCl) solutions. PEG feed concentration: 2 g L^{-1}; Symbols: experimental data; Full lines: intrinsic rejection rates computed from Eq. (9); (a): ceramic membrane; (b): polymeric membrane

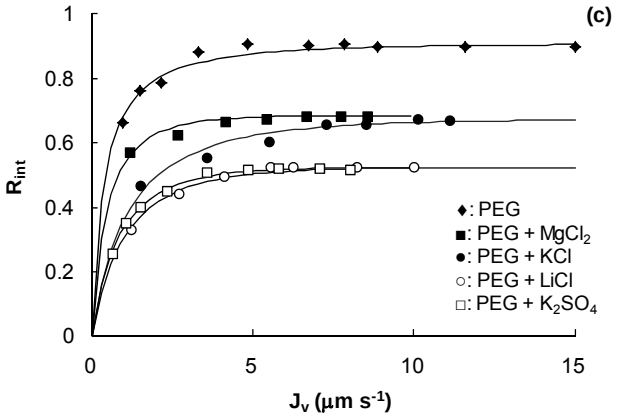

Fig. 3 Intrinsic rejection rate of PEG 600 vs. permeate volume flux for single-solute and mixed-solute solutions. PEG feed concentration: 2 g L^{-1}; Symbols: experimental data; Full lines: intrinsic rejection rates computed from Eq. (9); (a) ceramic membrane and salt concentration: 1 mol L^{-1}; (b): ceramic membrane and salt concentration: 0.1 mol L^{-1}; (c): polymeric membrane and salt concentration: 0.5 eq L^{-1}

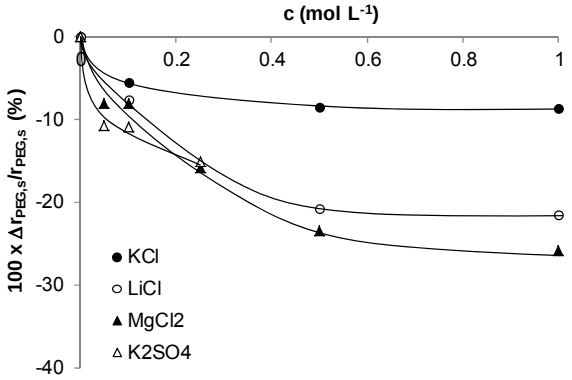

Fig. 4 Relative variation of the Stokes radius of PEG 600 vs. salt concentration in the various mixed-solute solutions. PEG feed concentration: 2 g L^{-1}; Ceramic membrane

Fig. 4 shows the relative variation of the effective size of the PEG 600 with the salt concentration of the various mixed-solute solutions. The Stokes radius of PEG 600 in single-solute solution was taken as 0.61 nm according to Afonso (2001). As can be seen, the salt effect varies from one salt to another. Regarding the effect of cations, the largest decrease in the effective size of PEG is obtained in the presence of $MgCl_2$ (~26% at 1 mol L^{-1}) and this reduction is larger for LiCl (~22% at 1 mol L^{-1}) than for KCl (~9% at 1 mol L^{-1}). As to the effect of anions, the effective size of PEG is found to decrease by ~6% and ~11% in the presence of KCl and K_2SO_4 at 0.1 mol L^{-1}, respectively. These findings are justified by the fact that the more ions are charged the more ions are hydrated, and the more ions are small (in terms of ionic radius) the more ions attract water molecules (due to a stronger electric field at the surface) and then, the number of water molecules that interact with the PEG 600 decreases. As expected, the salting-out effect depends on the ion concentration and also on both ion charge and ion size according to Hofmeister series.

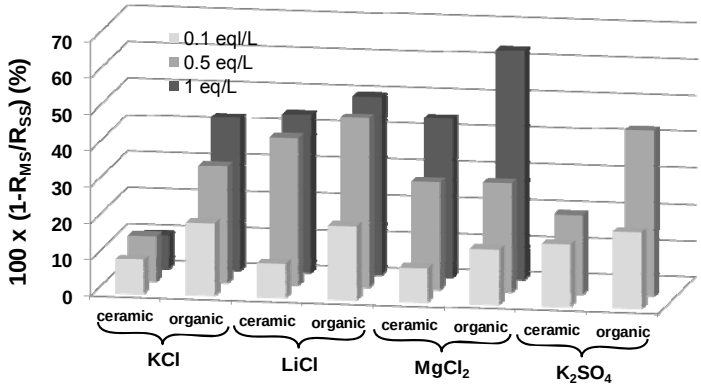

Fig. 5 Decrease of the limiting rejection rate of PEG 600 (expressed in %) in the presence of various salts at different concentrations for ceramic and polymeric membranes by comparison with the limiting rejection rate of PEG 600 in a single-solute solution. R_{SS}: limiting rejection rate of PEG 600 in a single-solute solution; R_{MS}: limiting rejection rate of PEG 600 in a mixed-solute solution

Unlike the ceramic membrane, the salting-out effect cannot be solely invoked with the polymeric membrane since the results obtained with this membrane are not in accordance with the Hofmeister series for cations and anions. Moreover, as shown in Fig. 5, the decrease in the limiting rejection rate is systematically higher for the polymeric membrane than for the ceramic membrane regardless of the salt and concentration. Since the salting-out phenomenon is independent of the membrane, the additional decrease observed with the polymeric membrane was then ascribed to the swelling of the pores. In order to evaluate the significance of the pore swelling phenomenon, the experimental data of rejection rates obtained with the polymeric membrane were used to compute the variation in the mean pore radius (and the membrane thickness-to-porosity ratio) in the presence of the various salts (the Stokes radii of PEG molecules in the presence of the various salts having been determined previously from rejection rates obtained with the ceramic membrane). Results show that the effective pore size depends on the salt nature and increases with salt concentration (Fig. 6). A variation from 7 to 31%, 19 to 50%, 16 to 59% and 14 to 51% is observed for $MgCl_2$, KCl, LiCl and K_2SO4, respectively, when concentration increases from 0.1 to 1 eq L^{-1} for the first three salts and from 0.1 to 0.5 eq L^{-1} for the last salt. No conclusion can be drawn at the lowest concentration. At 0.5 and 1 eq L^{-1}, the increase in the effective pore size is found to follow the order: K_2SO_4 > LiCl > KCl > $MgCl_2$ (K_2SO_4 could not be studied at the highest concentration). A number of studies have reported that the surface charge density depends on the salt nature and its concentration (Afonso 2001, Bruni 2008). The increase in the membrane charge density with the increasing salt concentration is believed to be caused by adsorption of ions from the solution onto the membrane surface. Thus, the addition of a salt in a solution could lead to an increase or decrease (in absolute value) in the surface charge density depending on the adsorbed ions, resulting in a greater or lower concentration of counterions inside pores to compensate the surface charge. This effect could lead to more or less important pore swelling depending on adsorbed ions, due to more or less strong electrostatic repulsions between counterions. The lowest increase in the effective pore size obtained with $MgCl_2$ and the greatest one observed with K_2SO_4 seem to support this assumption. Indeed, magnesium and sulfate ions,

which are known to specifically adsorb onto the membrane surface (Afonso 2001, Schaep 2001) could lead to lower membrane charge density (in absolute value) with $MgCl_2$ and to higher one (in absolute value) with K_2SO_4, in the case of a negatively charged membrane.

As for the influence of salt nature on the relative variation of the ratio $\Delta x/A_k$, no tendency could be observed due to overlapping of the experimental data for the various salts (results not shown).

4.3 Electrokinetic charge density of membranes

The salt effect on the membrane charge density was investigated by implementing coupled streaming potential coefficient ($\Delta\varphi_s/\Delta P$) and electric conductance (G_t) measurements. Zeta-potentials (ζ) were determined from Eq. (14) and then converted into electrokinetic charge density (σ_{ek}) according to Eq. (15). It should be noted that electrokinetic measurements have been carried out in salt solutions less concentrated than mixed-solute solutions so as to obtain a sufficiently high streaming potential. As shown in Fig. 7, the membrane is negatively charged regardless of the salt and the charge density increases (in absolute value) with salt concentration, probably due to an increasing adsorption of ions from the solution onto the membrane surface.

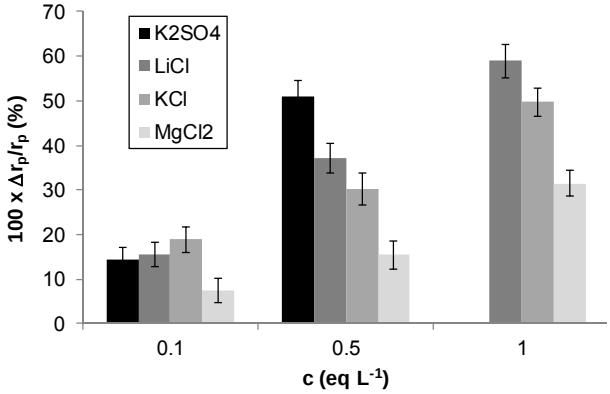

Fig. 6 Relative variation of the effective pore radius of the polymeric membrane as a function of salt concentration of mixed-solute solutions. PEG feed concentration: 2 g L^{-1}

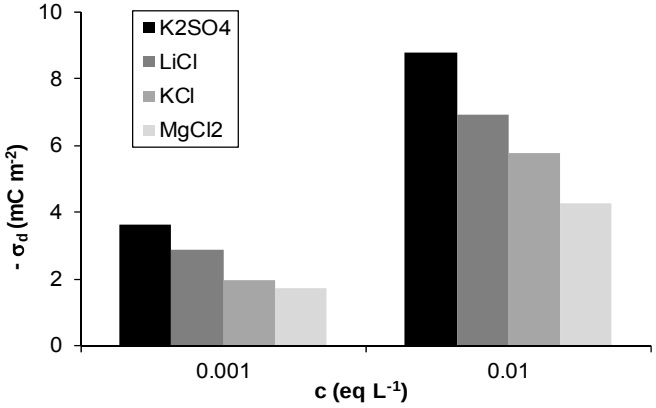

Fig. 7 Surface charge density of the polymeric membrane as a function of salt concentration

Concerning the effect of the salt nature, the surface charge density (in absolute value) follows the sequence: K_2SO_4 > LiCl > KCl > $MgCl_2$ at 0.001 and 0.01 eq L^{-1} (except for KCl and $MgCl_2$ which cannot be ranked at 0.001 eq L^{-1}). This charge density order is in accordance with that reported by Afonso (2001) with the same membrane and similar salts, i.e., Na_2SO_4 > NaCl > $MgCl_2$ (provided that Na^+ ions have the same influence on the membrane charging process as K^+ ions). It should be pointed out that the charge density order is strictly identical to the pore swelling order. If the salt effect on the membrane charge density is considered to be qualitatively the same at higher concentrations, it can then be concluded that the decrease of the PEG rejection in the presence of a salt is partly due to a pore swelling caused by an increase of the surface charge density.

4.4 Electrokinetic charge density of membranes

The salting-out and pore swelling effects on the transfer of PEG through the polymeric membrane could be decoupled by calculating the limiting rejection rate due to only salting-out effect. To this

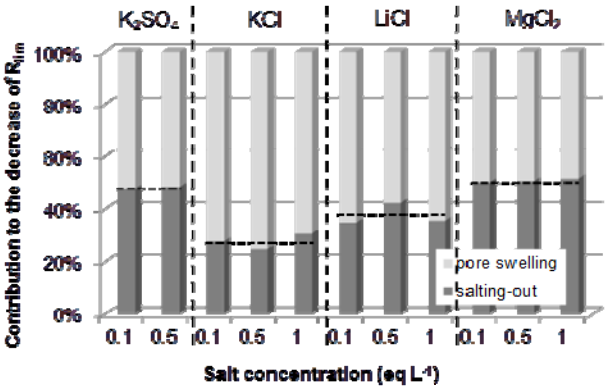

Fig. 8 Contribution of salting-out and pore swelling effects to the decrease in the limiting rejection rate of PEG 600 as a function of salt and concentration; polymeric membrane

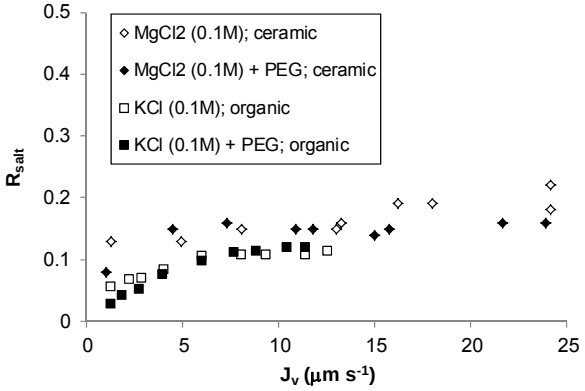

Fig. 9 Observed rejection rate of $MgCl_2$ (ceramic membrane) and KCl (polymeric membrane) as a function of permeate volume flux for single salt solutions and mixed-solute solutions (i.e., in the presence of PEG 600 at 2 g L^{-1})

end, the effective pore radius of the polymeric membrane in the absence of a salt (i.e., r_p = 0.875 nm) and the Stokes radii of PEG 600 in the presence of salts (assessed from rejection data measured with the ceramic membrane) were used in Eq. (10). Fig. 8 shows the contribution of the two phenomena – salting-out and pore swelling – to the decrease in the limiting intrinsic rejection rate of PEG. The contribution of the salting-out effect is found to be ~52% for $MgCl_2$, 35% for LiCl, 22% for KCl and 48% for K_2SO_4 and then it follows the Hofmeister series for both cations ($Mg^{2+} > Li^+ > K^+$) and anions ($SO_4^{2-} > Cl^-$), irrespective of salt concentrations. The dehydration of PEG molecules by ions is then also demonstrated in the case of the polymeric membrane. Both phenomena – dehydration and pore swelling – contribute similarly to the rejection rate drop in the presence of K_2SO_4 or $MgCl_2$ salts whereas the pore swelling becomes dominant in the presence of KCl or LiCl.

4.5 Impact of PEG on salt rejection

As illustrated by Fig. 9, the presence of PEG did not affect significantly the rejection of ions, for both ceramic and polymeric membranes, which is mainly controlled by electrostatic effects (Donnan exclusion and/or dielectric exclusion due to production of image forces). This finding is in accordance with result reported by Bouchoux (2001) with a polyamide NF membrane.

5. Conclusions

The influence of ions on the transfer of PEG through NF ceramic and polymeric membranes was studied. The main results obtained can be summarized as follows:

- The rejection of PEG molecules by both membranes significantly decreases when salts are added in the solution, and this decrease becomes more important as the ion concentration increases.
- For the ceramic membrane, it was found that the lowering of the PEG rejection rates follows the Hofmeister series for both cations and anions, i.e. $Mg^{2+} > Li^+ > K^+$, and $SO_4^{2-} > Cl^-$. The drop in the rejection rate was then ascribed to the partial dehydration of PEG molecules induced by the surrounding ions. This phenomenon was quantified by the determination of the variation of the effective size of the PEG. A decrease in the effective size of the PEG of 26%, 22% and 9% was observed in the presence of $MgCl_2$, LiCl and KCl at 1 mol L^{-1}, respectively, and of, 11% and 6% in the presence of K_2SO_4 and KCl at 0.1 mol L^{-1}, respectively.
- For the polymeric membrane, it was found that the salting-out effect cannot solely explain the rejection drop of PEG molecules in the presence of a salt since the decrease in the limiting rejection rate is systematically higher for the polymeric membrane than for the ceramic one. An additional phenomenon – the pore swelling – was then considered and quantified. Results show that the effective pore size depends on the salt nature and increases with salt concentration. It was found that the increase in the effective pore size can be as high as 59% in the case of LiCl at 1 mol L^{-1} (ou bien An increase in the effective pore size of 31%, 50%, and 59% was obtained in the presence of $MgCl_2$, KCl and LiCl at 1 eq L^{-1}, respectively, and of, 51% in the presence of K_2SO_4 at 0.5 eq L^{-1}. At 0.5 and 1 eq L^{-1}, the increase in the effective pore size was found to follow the following sequence: $K_2SO_4 > LiCl > KCl > MgCl_2$ (K_2SO_4 could not be studied at 1 eq L^{-1}). It should be noted that the effect of pore swelling modifies the Hofmeister sequence for cations. The hypothesis of pore swelling due to accumulation of counterions inside pores

resulting from an increase in the membrane charge was supported by electrokinetic charge density measurements since the charge density order was strictly identical to the pore swelling order.

• The contribution of both phenomena to the ion-induced decrease in the neutral solute rejection could be quantified. Remarkably, it was found that the contribution of the salting-out effect follows the Hofmeister series for both cations and anions, i.e. $Mg^{2+} > Li^{+} > K^{+}$, and $SO_4^{2-} > Cl^{-}$. The contribution is close to 50% for K_2SO_4 and $MgCl_2$ and less for KCl (~22%) and LiCl (~35%).

As a conclusion, the Hofmeister and pore swelling effects should be carefully considered in membrane-based purification processes since they are likely to affect the steric exclusion of neutral solutes when ions are in large quantities in the solution. The identification of the mechanisms involved in relationship with the transfer should allow to improve the prediction of the membrane processes performances and thus their implementation for different applications.

References

Afonso, M.D., Hagmeyer, G. and Gimbel, R. (2001), "Streaming potential measurements to assess the variation of nanofiltration membranes surface charge with the concentration of salt solutions", *Sep. Purif. Technol.*, **22-23**, 529-541.

Bargeman, G., Vollenbroek, J.M., Straatsma, J., Schroën, C.G.P.H. and Boom, R.M. (2005), "Nanofiltration of multi-component feeds. Interactions between neutral and charged components and their effect on retention", *J. Membr. Sci.*, **247**(1-2), 11-20.

Bouchoux, A., Roux-de Balmann, H. and Lutin, F. (2005), "Nanofiltration of glucose and sodium lactate solutions: variations of retention between single- and mixed solute solutions", *J. Membr. Sci.*, **258**(1-2), 123-132.

Bouranene, S., Szymczyk, A., Fievet, P. and Vidonne, A. (2007), "Influence of inorganic electrolytes on the retention of polyethyleneglycol by a nanofiltration ceramic membrane", *J. Membr. Sci.*, **290**(1-2), 216-221.

Bruni, L. and Bandini, S. (2008), "The role of the electrolyte on the mechanism of charge formation in polyamide nanofiltration membranes", *J. Membr. Sci.*, **308**(1-2), 136-151.

Fievet, P., Sbaï, M., Szymczyk, A. and Vidonne, A. (2003), "Determining the ζ-potential of plane membranes from tangential streaming potential measurements: Effect of the membrane body conductance", *J. Membr. Sci.*, **226**(1-2), 227-236.

Hunter, R.J. (1981), *Zeta potential in Colloid Science, Principles and Applications*, Academic Press, San Diego, CA, USA.

Kunz, W., Henle, J. and Ninham, B.W. (2004), "Zur Lehre von der Wirkung der Salze (about the science of the effect of salts): Franz Hofmeister's historical papers", *Curr. Opin. Colloid Interface Sci.*, **9**(1-2), 19-37.

Labbez, C., Fievet, P., Szymczyk, A., Aoubiza, B., Vidonne, A. and Pagetti, J. (2001), "Theoretical study of the electrokinetic and electrochemical behaviors of two-layer composite membranes", *J. Membr. Sci.*, **184**(1), 79-95.

Luo, J. and Wan, Y. (2011), "Effect of highly concentrated salt on retention of organic solutes by nanofiltration polymeric membranes", *J. Membr. Sci.*, **372**(1-2), 145-153.

Mandale, S. and Jones, M. (2008), "Interaction of electrolytes and non-electrolytes in nanofiltration", *Desalination*, **219**(1-3), 262-271.

Schaep, J., Vandecasteele, C., Wahab Mohammad, A. and Bowen, W.R. (2001). "Modelling the retention of ionic components for different nanofiltration membranes", *Sep. Purif. Technol.*, **22-23**, 169-179.

Szymczyk, A., Fatin-Rouge, N. and Fievet, P. (2007), "Tangential streaming potential as a tool in modelling

of ion transport through nanoporous membrane", *J. Colloid Interface Sci*., **309**(2), 154-160.
Yaroshchuk, A.E., Boiko, Y.P. and Makovetskiy, A.L. (2002), "Filtration potential across membranes containing selective layers", *Langmuir*, **18**(13), 5154-5162.
Zydney, A.L. (1997), "Stagnant film model for concentration polarization in membrane systems", *J. Membr. Sci*., **130**(1-2), 275-281.

ED

Greek symbols

δ	thickness of the polarization layer
$\Delta\varphi_s$	streaming potential
ΔP	hydrostatic pressure difference
Δx	effective thickness of the top layer
ε_0	vacuum permittivity
ε_r	effective dielectric constant inside pores
ϕ_i	steric partitioning coefficient for solute i
λ_i	ratio of the solute size to pore size ($\lambda_i = r_{i,s} / r_p$)
η	dynamic viscosity of the fluid
σ_{ek}	electrokinetic charge density
ζ	zeta potential

Nomenclature

A_k	porosity of the membrane top layer
c	salt concentration
c_i	concentration of solute *i* in the membrane
$c_{i,f}$	concentration of solute *i* in the feed solution
$c_{i,m}$	concentration of solute *i* at the membrane surface (at the membrane/feed solution interface)
$c_{i,p}$	concentration of solute *i* in the permeate
$c_i(0^+)$	concentration of solute *i* just inside the membrane pores (at the membrane/feed solution interface)
$c_i(\Delta x^-)$	concentration of solute *i* just inside the membrane pores (at the membrane/permeate interface)
$D_{i,\infty}$	bulk diffusion coefficient of solute *i* at infinite dilution
d_h	hydraulic diameter
F	faraday constant
G_t	total conductance
h	channel half-height
j_i	molar flux density of solute *i*
J_v	permeate volume flux
$K_{i,c}$	hydrodynamic coefficient accounting for the effect of pore walls on convective transport
$K_{i,d}$	hydrodynamic coefficient for hindered diffusion inside pores
$K_{i,s}$	hydrodynamics function
$K_{i,t}$	hydrodynamics function
k_B	boltzmann constant
k	mass-transfer coefficient *k*
l	channel length
L_c	channel width
Lp	pure water permeability
r_p	effective pore radius
$r_{i,s}$	stokes radius of solute *i*
R	ideal gas constant
Re	Reynolds number
R_{int}	intrinsic rejection rate
$R_{\mathrm{lim},int}$	limiting intrinsic rejection rate
R_{obs}	observed rejection rate
Sh:	Sherwood number
Sc:	Schmidt number
T	Temperature
x	coordinate
z_i	charge number of ion *i*